We are IntechOpen,
the world's leading publisher of
Open Access books
Built by scientists, for scientists

6,900
Open access books available

185,000
International authors and editors

200M
Downloads

154
Countries delivered to

Our authors are among the

TOP 1%
most cited scientists

12.2%
Contributors from top 500 universities

CLARIVATE ANALYTICS
BOOK CITATION INDEX
INDEXED

WEB OF SCIENCE™

Selection of our books indexed in the Book Citation Index
in Web of Science™ Core Collection (BKCI)

Interested in publishing with us?
Contact book.department@intechopen.com

Polyimides as High Temperature Capacitor Dielectrics

Janet Ho and Marshall Schroeder

Abstract

Nearly five decades of effort has focused on identifying and developing new polymer capacitor films for higher-than-ambient temperature applications, but simultaneous demands of processability, dielectric permittivity, thermal conductivity, dielectric breakdown strength, and self-clearing capability limit the number of available materials. Demands on these criteria are even more stringent in growing numbers of applications demanding high power performance. Aromatic polyimides, though not a panacea, are a class of heat-resistant polymers of great interest to researchers as capacitor dielectrics because of good thermal and mechanical stability. In this chapter, the key aspects and advantages of metallized polymer film capacitors are compared to analogous alternative technologies (polymer-film-metal-foil, ceramic, and electrolytic capacitors), followed by a comprehensive review of commercial resin development leading up to recent research on polyimides targeted for operating temperature above 150°C. Finally, this chapter provides a brief discussion on the recent effort on combining computation and synthesis to design polymers with desirable dielectric properties.

Keywords: Kapton, Ultem, polyimides, high temperature, capacitor dielectrics, thermal conductivity, self-clearing, metallized film capacitors, power electronics, DC link capacitors

1. Introduction

Capacitors are one of the primary components in power electronic devices, some of which are required to operate in hostile environments across a variety of consumer, industrial, and military sectors. For example, the sensors in "down hole" electronics for characterizing oil, gas, and geothermal wells can experience temperatures exceeding 200°C depending on the well depth. In the aircraft industry, new engine control systems require placement of sensor/actuator and signal conditioning electronics in or near aircraft engines where temperature can be in range of 200–300°C. Similar demands exist in the automobile industry, with power electronics located in the engine compartment and near the wheels of hybrid and electric vehicles where temperatures can reach 150°C [1–5].

For high voltage (>500 V [6]) applications, metallized polymer film capacitors are generally selected over polymer-film-metal-foil, ceramic, or electrolytic capacitors because of the enhanced volumetric efficiency and improved safety. Failure of a charged high energy capacitor (>10 kJ) is equivalent to a bomb, which requires design engineering with an appropriate failsafe mechanism such that energy is released gradually as the capacitor fails. Presently, the only compatible technology

is based on polymer film capacitors with thin metallization as electrodes, for which a thin layer of vacuum-deposited metallization (usually 20–100 nm of aluminum, zinc, or alloy [7]) functions as a fuse. When a localized breakdown of the film occurs during operation, (i) the current flowing through the breakdown site is limited by the metallization resistivity and (ii) the energy dissipated in the breakdown is sufficient to vaporize/oxidize the metallization near the breakdown, isolating the breakdown site. This results in a small decrease in capacitance but continued operation of the capacitor at the rated voltage. This "graceful" recovery mechanism is known as "self-clearing" and a photograph of a breakdown ("clearing") site in a metallized polymer film is shown in **Figure 1**. In contrast, polymer film capacitors with metal-foil electrodes (5–10 μm thick [9]) and ceramic capacitors, for which the electrode is a thick metal coating, often fail catastrophically if shorted [10, 11].

With power system designers striving for miniaturization and reliability at high temperatures and operating voltages, they must turn to specialized components.
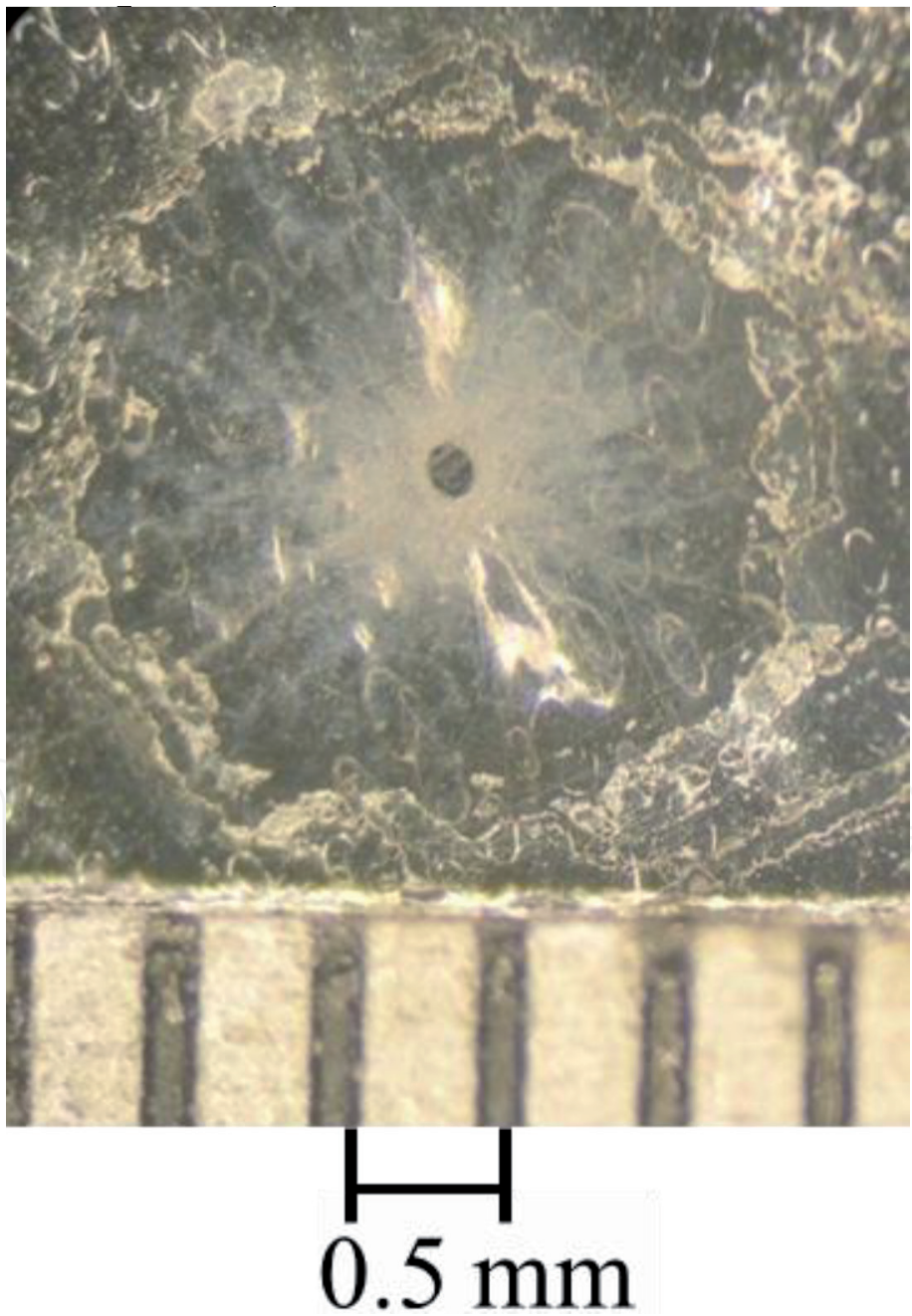
Figure 1.
Photograph of a breakdown site in a metallized polymer film. Figure reproduced from Figure 3 of [8] with permission from IEEE.

These applications are enabled, in part, by wide bandgap semiconductors (e.g., silicon carbide), which support operation at temperatures well above 150°C [3, 12]. However, these types of environments are too aggressive for conventional polymer capacitor dielectrics unless the voltage is derated, or an active cooling mechanism is implemented, introducing additional cost and complexity while reducing energy efficiency. High temperature polymer film capacitors offer a promising solution for these issues due to reduced thermal management requirements and elimination of the voltage derating due to improved stability of the breakdown strength at high temperatures. Aromatic polyimides are one specific class of high temperature polymers which have been commercially available since the early 1960s [13], but the form in which these materials are manufactured generally does not meet the specifications required for capacitor films. One of the main requirements is the processability of the polymer into a continuous thin film (<12 μm thickness), since the capacitance scales inversely with film thickness [14]. This limitation precludes the use of Kapton® polyimide as a capacitor dielectric [15], even though it has been used extensively as wire and cable insulation for aircraft with a continuous operating temperature of 300–350°C since the early 1980s [16–18].

One major impediment to the development and integration of new capacitor dielectrics is that specialty film chemistries optimized specifically for high performance polymer capacitors represent relatively small markets (i.e. military, aerospace, and down hole exploration [3, 12]) compared to those necessary for profitable commercial production of a polymer resin. Other than biaxially oriented polypropylene (BOPP) and polyethylene terephthalate (BOPET), which are commodity films in a variety of commercial applications such as packaging [19, 20], nearly all commercial polymer capacitor films are specialty polymers synthesized for other applications. For example, poly (phenylene sulfide) (PPS) and poly(ethylene 2,6-naphthalate) (PEN) are available as premium capacitor dielectrics, but the majority of their use is in automotive, household, and food packaging applications [21–24].

This chapter discusses the important criteria for high temperature polymer capacitor dielectrics and presents a comprehensive review on commercial resin development up to recent research progress on polyimide (PI) targeted for operating temperature above 150°C. While many review articles on various aspects of polymeric capacitor dielectrics are available [25–32], this chapter has a specific focus on polyimides for high temperature applications.

2. Relevant polymer properties for capacitors dielectrics

The deliverable energy density of a capacitor scales linearly with the dielectric constant and quadratically with breakdown strength. As such, engineers and scientists often focus on these two properties while neglecting other relevant characteristics, such as thermal conductivity and the implications of chemical composition of a polymer on self-clearing capability. These properties will be discussed in the following subsections.

2.1 Thermal conductivity

For reliable operation at elevated temperatures, efficient heat removal from the interior of capacitors is essential but often challenging, especially in metallized polymer film designs due to the low thermal conductivity of both the polymer dielectric and the thin metallization [33]. As electrical insulators, polymer dielectrics are poor thermal conductors with thermal conductivities ranging from

0.1 W/(m·K) for amorphous polymers [34] to about 0.6 W/(m·K) for the present state-of-the-art BOPP capacitor films [35]. As for the electrodes, while the thermal conductivity of metals are typically three orders of magnitude higher than those of polymers, the metallization is also ~1000 times thinner than the dielectric and may not have the thermal conductivity of the bulk metal from which it is deposited. One approach to increase thermal conductivity of the polymer is by blending in ceramic nano-fillers. Researchers have shown that mixing 10 vol% boron-nitride nano-sheets (BNNS) with an amorphous polymer resulted in a six-fold increase in thermal conductivity from 0.3 to 1.8 W/(K·m) [36]. The resulting BNNS/polymer nanocomposite also exhibited an increase in dielectric constant, breakdown strength, and charge-discharge efficiency, the latter of which was attributed to reduction of the conduction current. A similar trend has also been observed in other polymer systems including polyimides [37, 38].

2.2 Self-clearing capability: implications of chemical composition

For a self-clearing event to occur successfully, the metallization needs to be thin enough to be vaporized/oxidized by the energy dissipated during the dielectric breakdown. In addition, the polymer also needs to be oxidized completely, leaving no conductive paths from free carbon in the region of cleared metallization around the breakdown site, as shown in **Figure 1** [8]. Based on an in-depth study of the physics and chemistry of clearing phenomena, polymers with low ratios of carbon to (hydrogen + oxygen) in the repeating units, such as cellulose, often exhibit excellent self-clearing. Conversely, polymers with high carbon to (hydrogen + oxygen) ratios, like polystyrene, tend to form greater amounts of free carbon for a given clearing energy and clear poorly [7]. This trend is illustrated in **Table 1**,

Polymer	Repeating unit	C	O	H	N	S	$\frac{(C+N+S)^a}{(H+O)}$	Carbonization [b] (Calc.) %	Carbonization [b] (Meas.) %	Self Clearing [c]
Cellulose		6	5	10	0	0	0.40	2	2.2	excellent
Cellulose Acetate		10	7	14	0	0	0.48	5	3	excellent
Polypropylene		3	0	6	0	0	0.5	54	50.5	good
Polyethylene terephthalate		10	4	8	0	0	0.83	41	37.5	medium
Polycarbonate		16	3	14	0	0	0.94	60	58.5	--
Polyethylene naphthalate		14	4	10	0	0	1.0	N/A	N/A	medium-low
Polystyrene		8	0	8	0	0	1.0	76	75.5	low
Polyphenylene sulfide		6	0	5	0	1	1.4	N/A	N/A	low
Kapton polyimide		22	5	10	2	0	1.6	N/A	N/A	--

[a]*Adapted from [5].*
[b]*Data taken from [7].*
[c]*Observation taken from [5, 7].*

Table 1.
Chemical composition of various polymer dielectrics including ratios of (carbon + nitrogen + sulfur) to (hydrogen + oxygen), amount of residual carbon, and the observation of self-clearing behavior.

in which the chemical composition of various polymer dielectrics is correlated with the amount of carbon residue, both measured and calculated, based on comparison between amount of carbon in the gaseous by-products and composition of the dielectrics [5, 7]. Kapton® polyimide, also shown in **Table 1**, has a high degree of aromaticity in the structure and has a tendency toward carbonization (arc-tracking), as observed in wire insulation in commercial aircraft before fluoropolymers were applied as thin coatings to resist arc-tracking [39, 40]. Poor self-clearing can be mitigated to some degree by applying a thin coating of acrylate over the dielectric to increase the oxygen content. The clearing energy can also be reduced by increasing the metallization resistance in order to avoid damaging adjacent layers of dielectric during clearing (**Figure 2**), given that a metallized film capacitor is typically wound from two layers of single-side-metallized dielectric film as illustrated in **Figure 3** [8]. However, the trade-offs for increasing metallization resistance include higher equivalent series resistance (ESR), lower thermal conductivity, and lower ripple current handling capability. Thus, achieving an optimum balance between capacitor ESR and clearing energy depends on the application requirements.

2.3 Tensile strength

In order to withstand the tension applied by winding machines during capacitor manufacturing, a polymer dielectric must have sufficient tensile strength. A typical value of tension used by capacitor manufacturers is about 10 MPa while the typical tensile strength for various commercially available capacitor films is in the range of 160–200 MPa [41]. In comparison, Kapton® polyimide has a tensile strength of 72 MPa and poly(ether imide) 97 MPa [31]. Based on these values, the tensile strengths of the polymers discussed herein are sufficient for capacitor winding.

## 2.4 Temperature dependence of dielectric constant, dissipation factor, and breakdown strength

Polar polymers often exhibit a substantial increase in dielectric constant when the temperature passes through the glass transition temperature (T_g) of
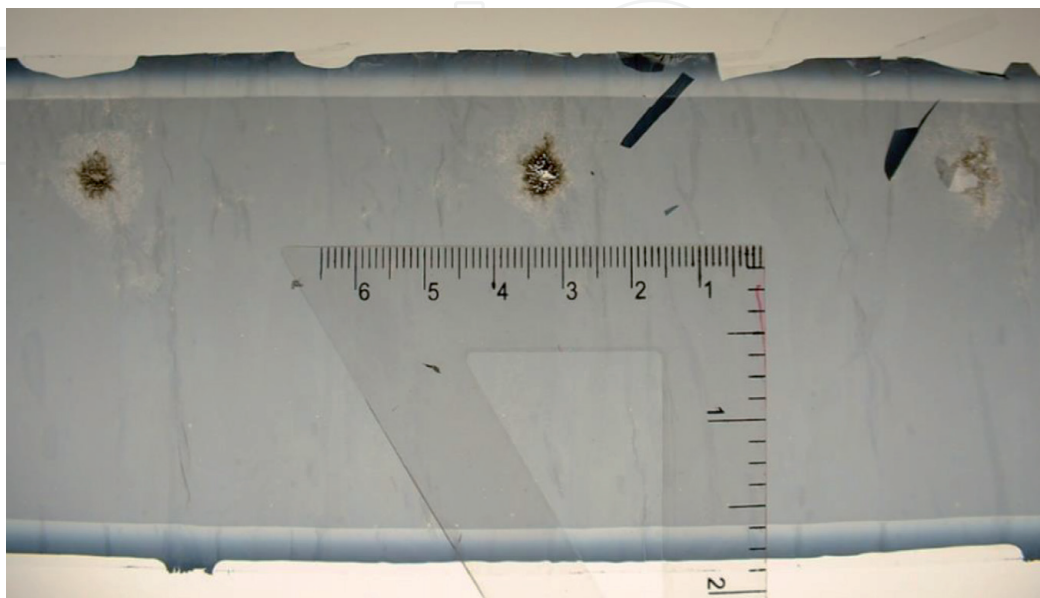
Figure 2.
Photograph of an unwound metallized film capacitor having poor self-clearing behavior with damage involving adjacent layers.
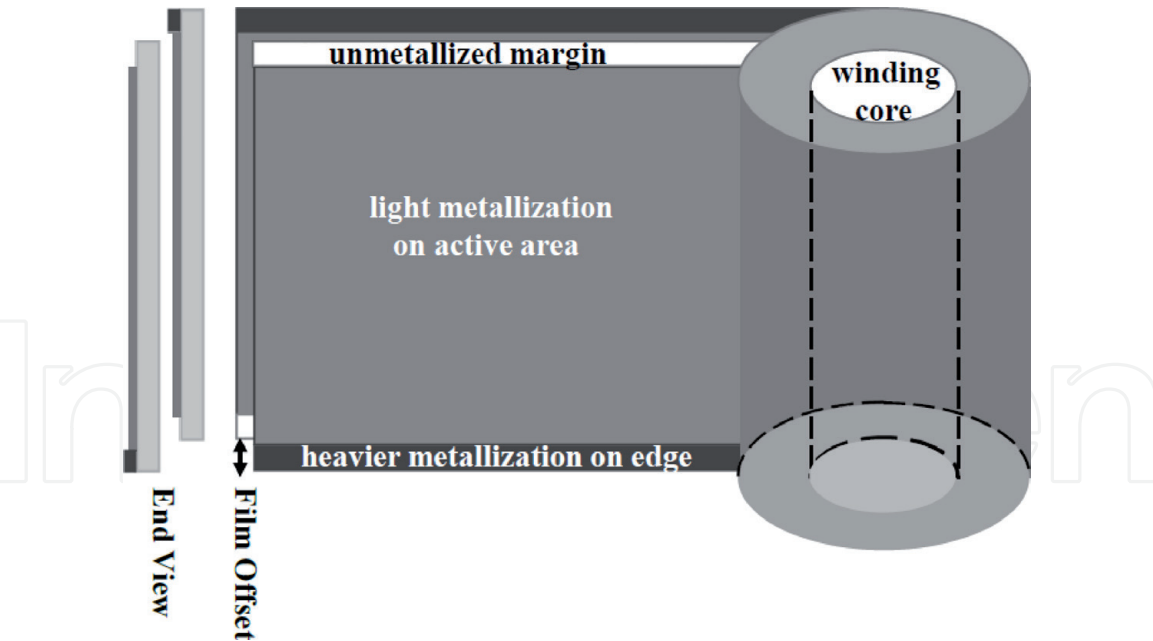
Figure 3.
Schematic of the construction of a metallized polymer film capacitor winding without the end connections.
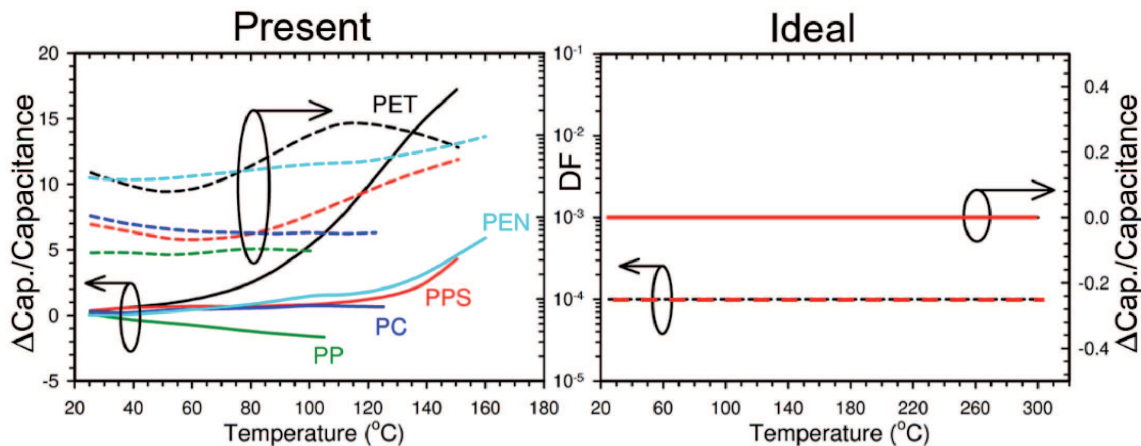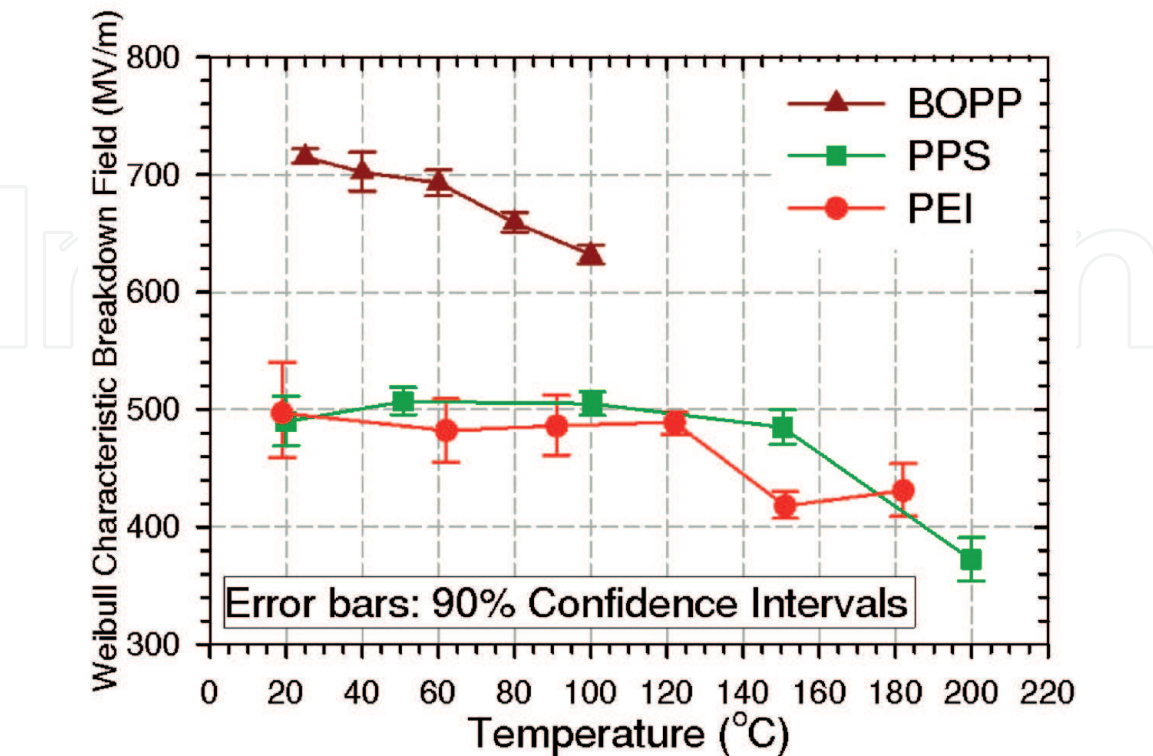

Figure 4.
Typical change in capacitance and dissipation factor (DF) of various polymer film capacitors as a function of temperature at 1 kHz. PET: poly(ethylene terephthalate), PEN: poly(ethylene 2,6-naphthalate), PPS: poly(phenylene sulfide), PC: poly(carbonate), PP: poly(propylene). Data adapted from [42, 43].

the polymer; however, non-polar polymers, which have only electronic polarization, are less temperature-dependent (**Figure 4**). The temperature dependence of dielectric constant for polar polymers is the result of increased polymer chain mobility as temperature increases through the T_g. This leads to greater freedom in accessible molecular dipole orientations at frequencies below 10^{12} Hz, while the electronic and atomic contributions tend to occur at around 10^{12} Hz and above [44]. Furthermore, polymers tend to have a broad distribution of response times as a result of interconnectivity and steric-hindrance imposed by neighboring molecules [45]. Substantial increases in dielectric constant near T_g limit capacitor operation for polar dielectrics to somewhat below T_g for many applications requiring a stable capacitance, including power conditioning/conversion in electronic circuitry, where the operating frequency ranges from tens of kHz for silicon-based switches to a few GHz for gallium nitride transistors [46].

Dissipation factor (DF) of a dielectric is a measure of electrical energy dissipated, usually in the form of heat, when an oscillating electric field is applied.

Similar to the dielectric constant, the DF is temperature and frequency-dependent and is more pronounced for polar polymers (**Figure 4**). In a capacitor, the total DF is a combination of contributions from the electrode and the polymer. For the electrode, metallization has a characteristic DF of ~0.1%, while the DF of metal foils is negligible. For polymers, DF can range from 0.01% for nonpolar polymers like PP, to as high as 1% for polar polymers such as PET, as shown in **Figure 4**. Depending on the capacitor applications, such as in a snubber or DC link, the requirement for dissipation factor ranges from ~0.01% for the former, to 0.1% for the latter [47–50]. Thus, for a snubber to meet the low DF requirement, metal foil electrodes with a BOPP polymer film is a common capacitor configuration.

The breakdown strength of a dielectric is defined as the maximum electric field that a dielectric can sustain for a given electrode configuration, test area, [51, 52] and voltage waveform (e.g. linear voltage ramp rate for DC breakdown [53]). The breakdown field is a statistical parameter, typically characterized by a Weibull distribution, although sometimes the log-Normal distribution provides a better fit [54]. It is usually determined by extrinsic factors such as weak points or defects such as embedded foreign particles in the dielectric [55]. Therefore, when reporting the breakdown field at the film level (as opposed to a wound capacitor), measurement conditions such as the electrode configuration (ball-plane or parallel plates) and test area should be included. For comparison purposes, all breakdown field data contained in this chapter included a description of the measurement conditions or control measurements with other capacitor-grade polymer films. Presently, BOPP capacitor films have the highest breakdown field of ~700 MV/m (at the 63% Weibull cumulative probability for a test area of ~2 cm^2 and 300 V/s linear ramp voltage) among all commercial polymer capacitor films [56]. The breakdown field of polymers decreases as temperature approaches T$_g$ of amorphous (e.g. poly-ether-imide or PEI) or T$_m$ of semi-crystalline polymers, [such as BOPP and BO poly-phenylene-sulfide

Figure 5.
Weibull characteristic breakdown field as a function of temperature for various polymers. Electrode area: ~2 cm². BOPP: biaxially oriented poly(propylene), PPS: poly(phenylene sulfide), PEI: poly(ether imide). Figure taken from [57].
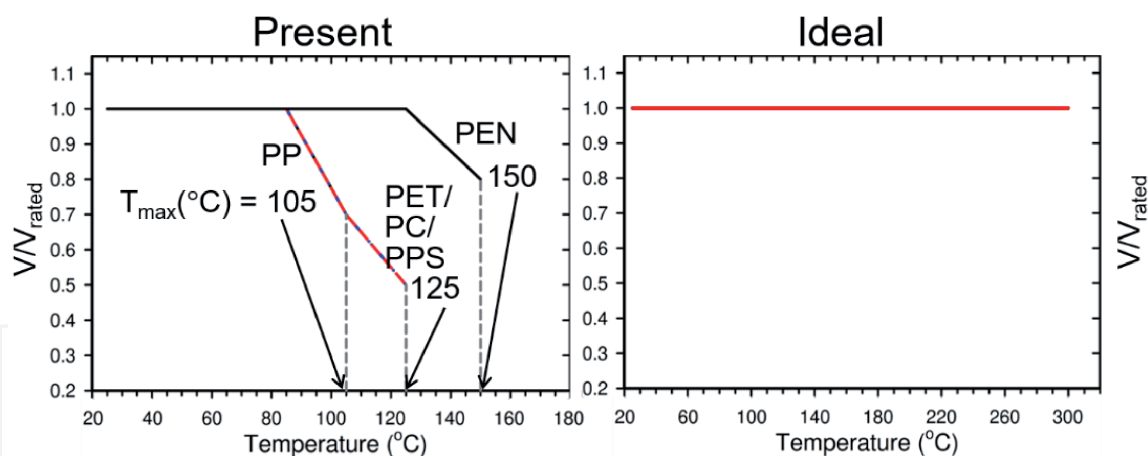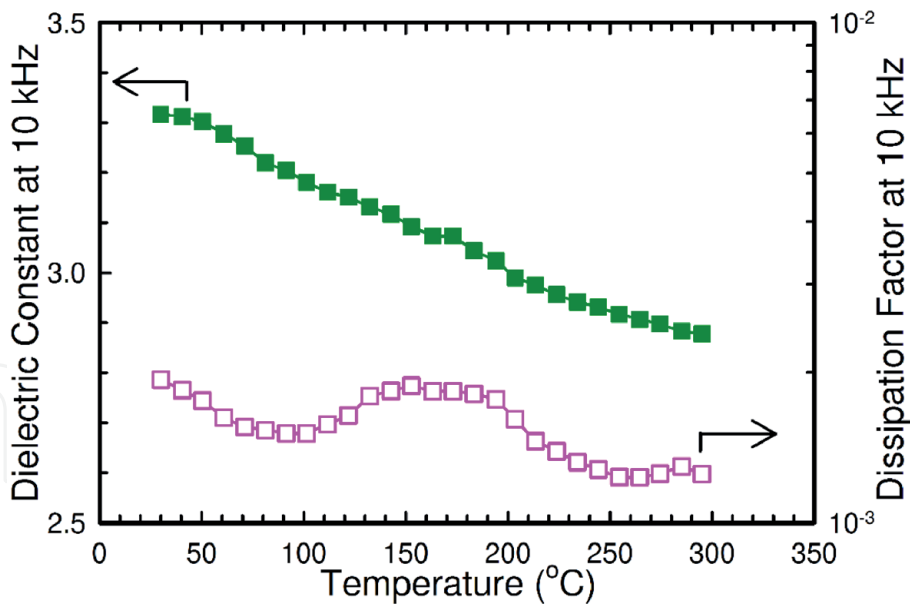
Figure 6.
Typical derating of operating voltage for various polymer film capacitors as a function of temperature.
PET: poly(ethylene terephthalate), PEN: poly(ethylene 2,6-naphthalate), PPS: poly(phenylene sulfide), PC:
poly(carbonate), PP: poly(propylene). Data adapted from [42, 43].

(PPS)], as shown in **Figure 5** [57]. Hence, the operating voltage of a capacitor is usually derated at elevated temperatures to protect against failure and prolong operational lifetime (**Figure 6**). Although many breakdown mechanisms have been proposed [58–61], extrinsic breakdown in solids is generally driven by power dissipation and eventually "thermal runaway", which leads to breakdown [62, 63].

3. Commercial polyimides evaluated for capacitor applications

In the early 1990s, the lack of suitable high temperature polymer film capacitors prompted a concerted effort funded by NASA and the U.S. Air Force to develop new capacitor dielectrics based on commercially available heat-resistant polymers with operating temperatures above 200°C. While Kapton® polyimide has been used extensively since the early 1980s as wire and cable insulation for aircraft (continuous operating temperature of 300–350°C [16–18]), it has never been used as a capacitor dielectric due in part to its previous inability to be manufactured in thin films. Nevertheless, it is a common benchmark for development of new dielectrics. One study reported that the dissipation factor of Kapton® at the film level increased from 0.1% at 25°C and 1 kHz to 6% at 300°C, while that the dielectric constant decreased from 3.1 at 25°C and 1 kHz to 2.8 at 300°C [64, 65]. At 10 kHz, Kapton® showed a similar decreasing trend with increasing temperature for the dielectric constant while the dissipation factor remained constant at 0.1% at temperature up to 300°C, as shown in **Figure 7** [36]. Another recent study showed that Kapton® at 1 kHz in a film-foil capacitor configuration exhibited a gradual decrease in capacitance from 25 up to 225°C, followed by an abrupt increase at higher temperature, as illustrated in **Figure 8**. In this configuration, the dissipation factor of Kapton® remained constant at 0.1% up to 200°C and then increased sharply as temperature was further increased [66].

Another aromatic polyimide is SIXEF-44™ (**Figure 9**), which is manufactured by Hoechst Celanese based on 2,2-bis(3,4dicarboxyphenyl) hexafluoropropane dianhydride (6FDA) and 2,2-bis(4-aminophenyl) hexafluoropropane diamine (4,4′-6F diamine). This fluorinated polyimide has a glass-transition temperature (T_g) of 323°C [67] and a dielectric constant of 2.8 at 1 kHz with <10% change across temperature range from −55 to 300°C. The dissipation factor is around 0.1% over the temperature range of 25–250°C from 100 Hz to 10 kHz, as illustrated in

Figure 7.
Dielectric constant and dissipation factor at 10 kHz for Kapton® film as a function of temperature. Data adapted from [36].
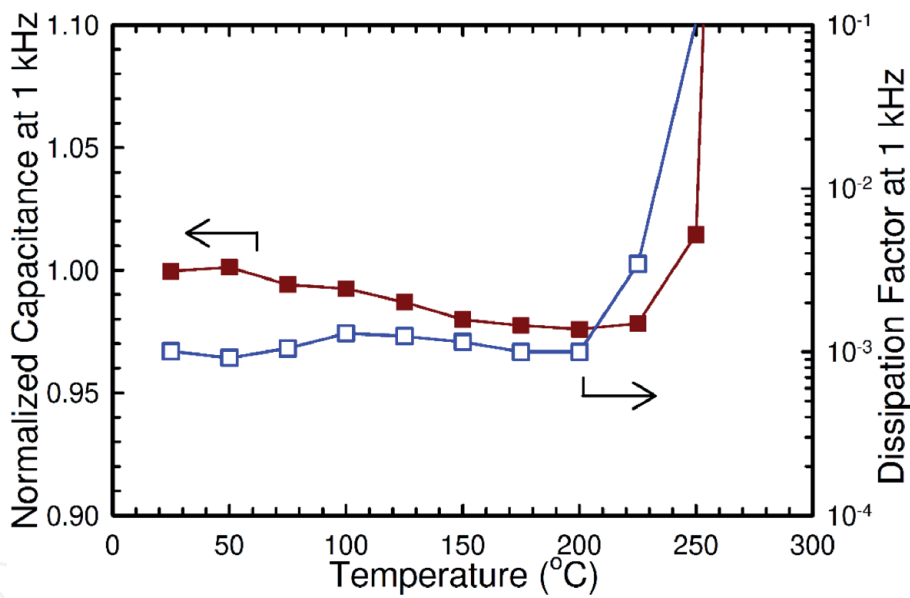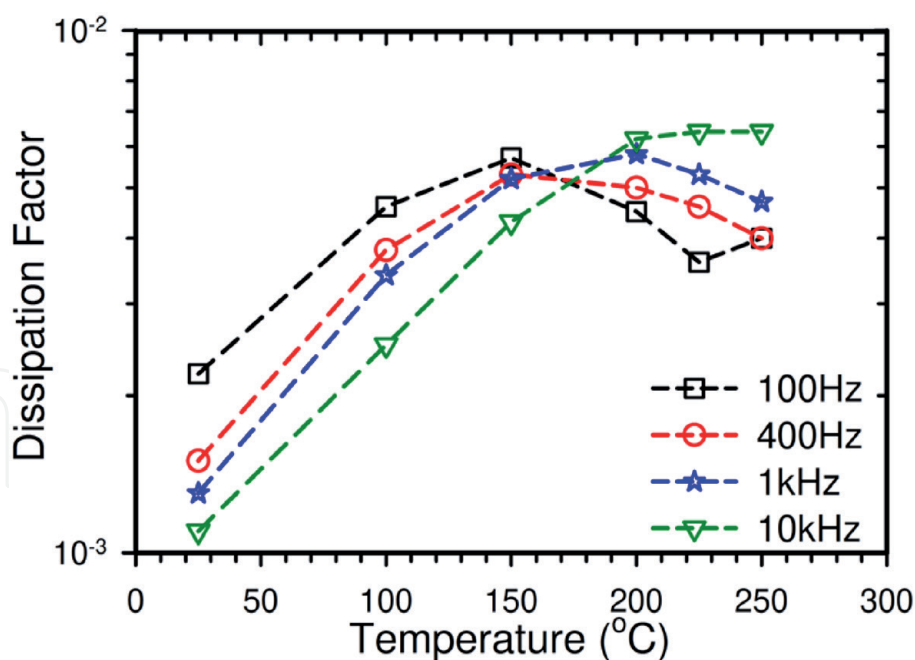

Figure 8.
Normalized capacitance and dissipation factor at 1 kHz as a function of temperature for an 8-μm Kapton® HN-30 film capacitor wound with 12-μm copper foil. Data adapted from [66].
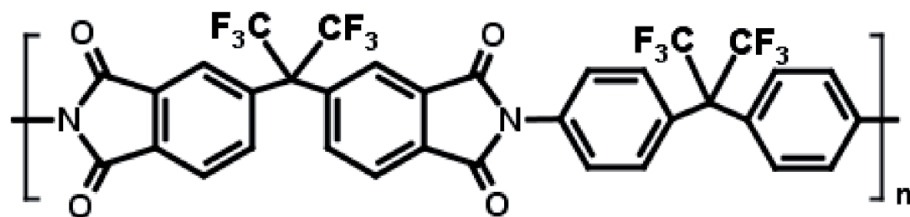
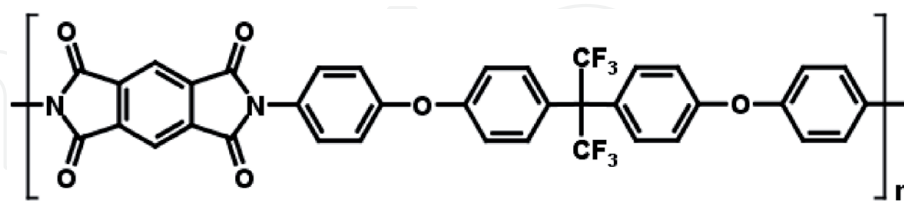**Figure 9.**
Chemical structure of SIXEF-44™.

Figure 10 [68]. The reduced dielectric constant in SIXEF-44™ relative to nonfluorinated counterparts was attributed to the symmetry of the fluorine atoms on the polymer backbone [67, 69, 70].
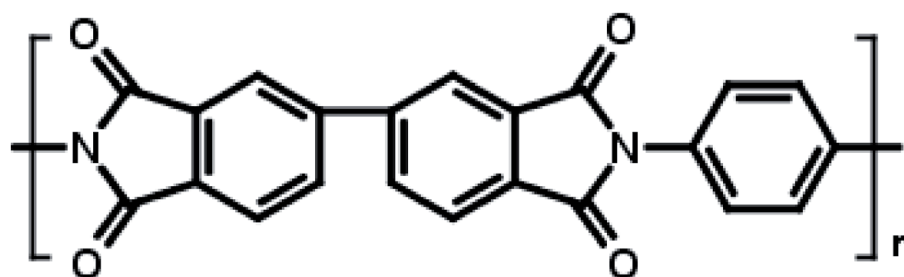
Figure 10.
Dissipation factor of SIXEF-44™ as a function of temperature at various frequencies. Data adapted from [68].

Other aromatic polyimides investigated include perfluoropolyimide (PFPI) (**Figure 11**) and Upilex-S® (**Figure 12**). PFPI was developed by TRW, Inc., and is a perfluoroisopropylidene diamine of 2,2-bis(4,4-aminophenoxy)-phenyl-hexafluoropropane (4-BDAF) and pyromellitic dianhydride (PMDA) [71]. Upilex-S® was originally synthesized by ICI Americas, Inc. from monomers of 3,3′,4,4′-biphenyl tetracarboxylic dianhydride (BPDA) and p-phenylene diamine (p-PDA). The T_g for PFPI is above 390°C [72] while that of Upilex-S® is 355°C [73]. The dielectric constant of PFPI is 3.1 at 25°C but decreases to 2.9 at 300°C [64, 65], while that of Upilex-S® is 3.3 for 1 kHz and temperatures from 25 to 300°C. The dissipation factor for both PFPI and Upilex-S® at 1 kHz is about 0.1% at both 25 and 300°C.
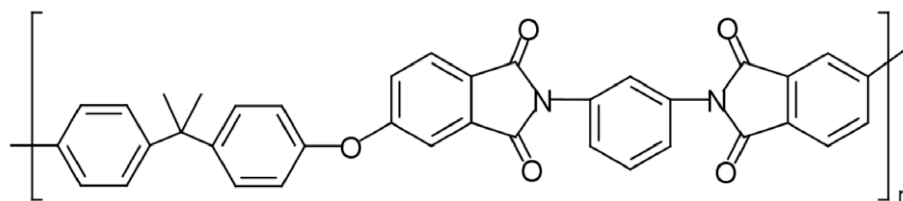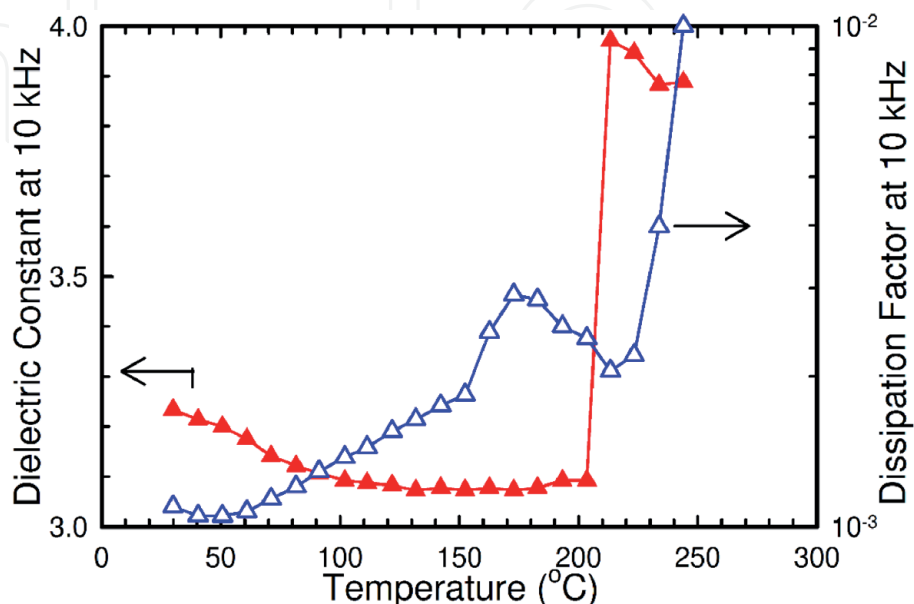

Figure 11.
Chemical structure of PFPI.

Figure 12.
Chemical structure of Upilex-S®.

Figure 13.
Chemical structure of PEI.

Figure 14.
Dielectric constant and dissipation factor at 10 kHz for PEI film as a function of temperature. Data adapted from [36, 57].

Most aromatic polyimides suffer from the same processing issues as a result of the high degree of aromaticity, which led researchers to develop modified systems with flexible moieties such as ether linkages and alkyl groups in the polymer backbone. One example is Ultem™, which is poly(ether imide) (PEI) (**Figure 13**) that is synthesized from the disodium salt of bisphenol A and 1,3-bis(4-nitrophthalimido)benzene [74]. Subsequent development efforts focused on melt-extrusion and stretching of PEI films have enabled film thicknesses as thin as 5 μm [31]. The T_g of PEI is ~215°C, which is considerably lower than many of the wholly aromatic polyimides due to the increase in flexibility imparted by the ether linkages and alkyl groups [17]. The dielectric constant and dissipation factor of PEI are about 3.1 and 0.2%, respectively, at frequencies from 100 Hz to 10 kHz and temperatures from 25 to 200°C; however, they increase sharply as temperature approaches the T_g, as shown in **Figure 14** [36, 57]. Such temperature dependence for the dielectric constant and dissipation factor is a characteristic for polymers with molecular dipoles as discussed in Section 2.4.

4. Recently developed polyimides

Over the past 10 years, research efforts have continued to develop new polyimides for capacitor dielectrics. The thermal stability of these new polymers is primarily derived from a high degree of aromaticity and fused-ring heterocyclic rigid structures. As energy density of a capacitor scales with the dielectric constant, some researchers have specifically focused on designing new aromatic polyimides

(PIs) that have a higher dielectric constant than the typical value of 3 while preserving the essential thermal/mechanical properties.

One common approach to increasing the dielectric constant is by incorporating polar moieties into the backbone of a polymer chain to enhance the dipole moment. The nitrile group (—CN) is one of the polar moieties that was explored by Wang et al. [75, 76] and Treufeld et al. [77], in which the number of —CN dipoles on the diamine was varied between 0, 1, and 3. The nitrile-containing diamines synthesized in the study were aminophenoxy-benzonitrile (APBN)-based with the two amino groups varying between three isomeric positions (m,m, m,p, and p,p) (**Figure 15**) to explore the effect of isomeric position on the 6FDA-based PIs. A nitrile-free analog, LaRC-CP2™ [78, 79], was used as a control.

Among the 6FDA-based PIs, the addition of one nitrile group in the diamine increased the room temperature dielectric constant from 2.9 (independent of frequency between 0.1 Hz and 1 MHz for the nitrile-free PI) to between 3.1 and 3.5 depending on the frequency and isomeric positions of the diamine linkage. In general, the m,m- and m,p-positions exhibited higher values (3.25–3.5) as compared to the p,p-position (**Figure 16**). Further increasing the nitrile content to three nitrile groups per diamine monomer resulted in an additional increase of the room temperature dielectric constant to between 3.5 and 3.7 (frequency dependent) for the 6FDA-based PIs with p,p-linkage. Interestingly, substitution of the other two isomeric positions had no significant effect (**Figure 17**). The investigators explained that the greater flexibility of the three —CN dipoles in the p,p-linkage as compared to the m,m- or m,p-linkage in the diamine resulted in greater dipolar polarization. An increase in dielectric constant was also observed in the OPDA-based PIs with m,m diamine linkage with increasing content of —CN dipoles.
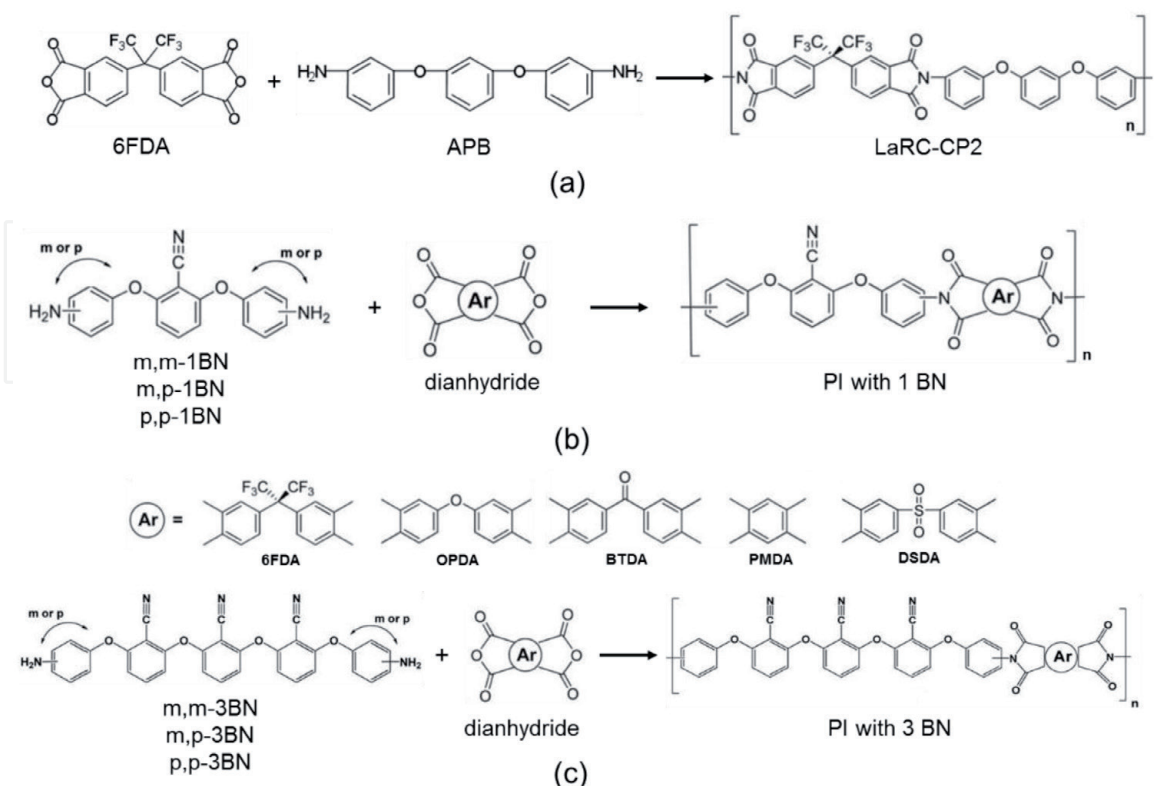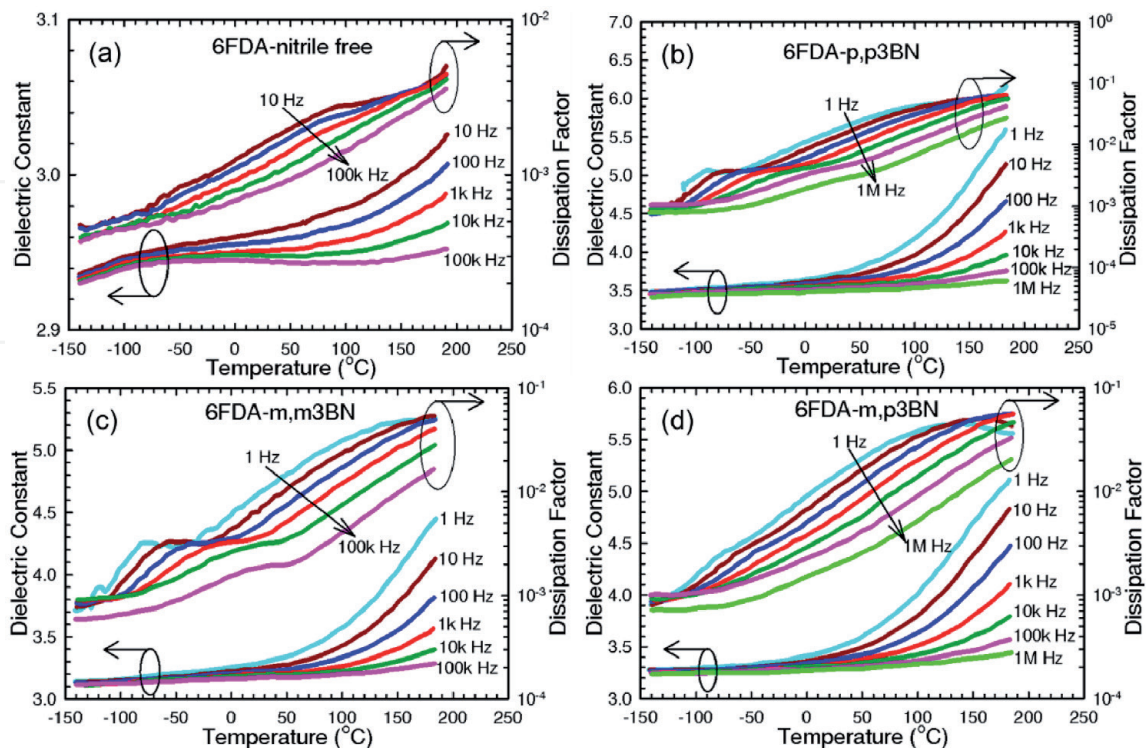

Figure 15.
Reaction schemes of various polyimides: (a) LaRC-CP2 from 2,2-bis(phthalic anhydride)-1,1,1,3,3,3-hexafluoroisopropane (6FDA) and the 1,3-bis(3-aminophenoxy) benzene (APB) diamine, (b) with one benzonitrile (BN) group, (c) with three benzonitrile groups. Reaction schemes adapted from [75, 76].
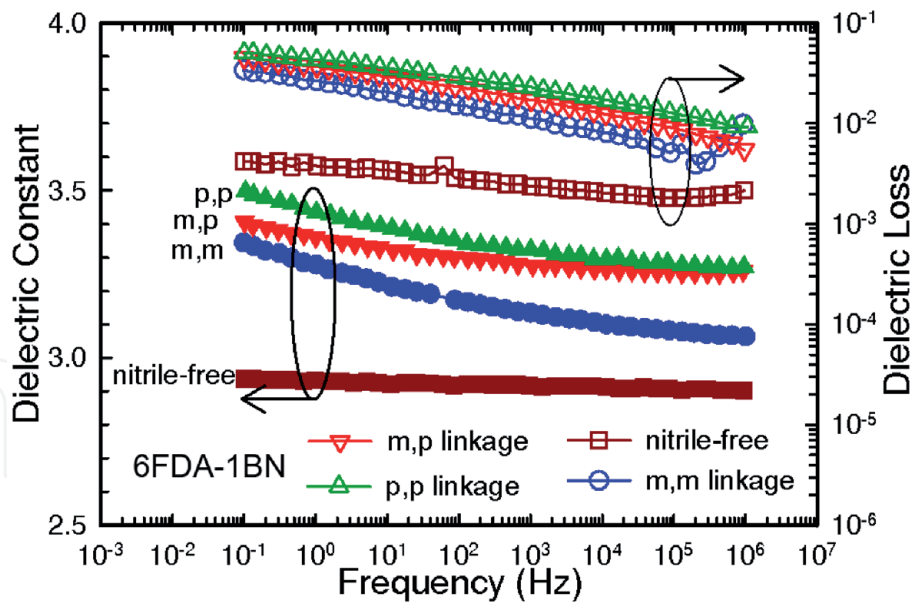
Figure 16.
Dielectric constant and dielectric loss as a function of frequency at ambient conditions for 6FDA-APB nitrile free PI and the three analogs containing one ━CN dipole per diamine at different isomeric positions. Data adapted from [75].

The key drawback of the addition of nitrile groups was the increase in temperature dependence in both the dielectric constant and dissipation factor, as illustrated in **Figure 17**. For example, the dielectric constant of the nitrile-free 6FDA-based PI at 10 kHz increased by only 1.4% over a temperature range of −150 to 190°C, whereas that of the three nitrile-containing analogs with the m,m-, p,p-, and m,p-linkages rose 6.3, 8.3, and 15%, respectively. With respect to the dissipation factor, the nitrile-free PI remained below 0.5% over the tested temperature/frequency
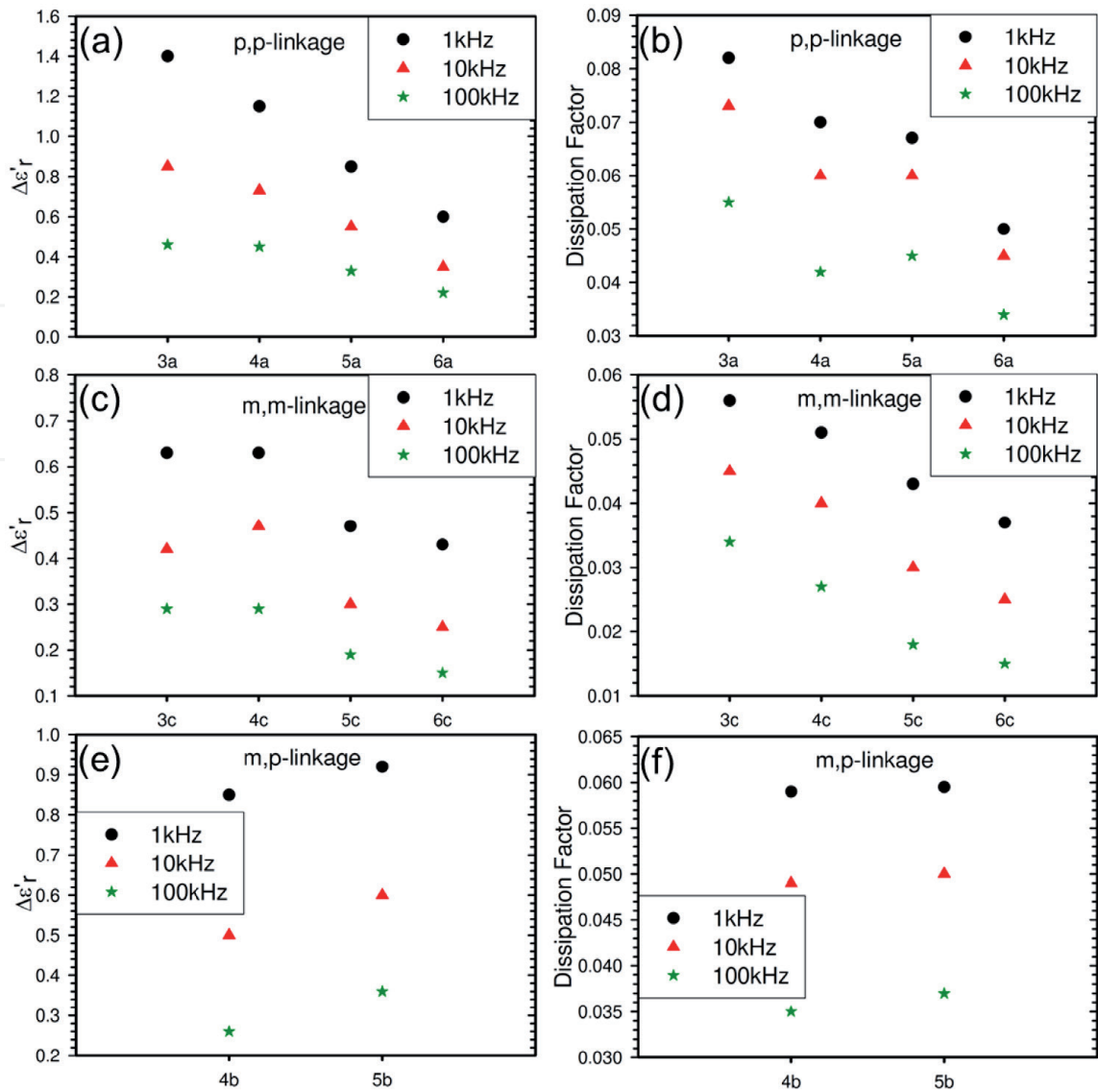

Figure 17.
Dielectric constant and dissipation factor as a function of temperature at various frequencies for the 6FDA-based PIs containing three nitrile groups in different isomeric positions (a–c) and the nitrile-free analog, LaRC-CP2 (d). Data taken from [77].

range, while the same nitrile-containing PIs increased from below 0.1% at −150°C to above 1% at 190°C between 10 Hz and 100 kHz. The temperature scan was limited to 190°C to avoid deforming the sample significantly. The investigators attributed the increase in dielectric constant with temperature at high frequencies to increased short-range segmental motion as the T_g was approached, which resulted in stronger dipolar polarization. However, since the ▬CN dipoles were attached to the polymer backbone in a 90° configuration, the segmental motion was hindered, causing friction with the neighboring chains and leading to high dissipation factor at high temperatures and frequencies. At low frequencies (<10 Hz), the increase in dielectric constant and dissipation factor with temperature was attributed to ions present from residual solvent and unreacted poly(amic acid) precursors in the 35–50 μm thick samples.

The investigators also compared the structural effect of four dianhydrides on the dielectric properties of PIs with three ▬CN dipoles in the diamine unit. The four dianhydride monomers under study were 2,2-bis(phthalic anhydride)-1,1,1,3,3,3-hexafluoroisopropane (6FDA), 4,4′-oxydiphthalic dianhydride (OPDA), 4,4′-benzophenonetetracarboxylic dianhydride (BTDA), and pyromellitic dianhydride (PMDA). The chemical structures of these dianhydrides are shown in **Figure 15**. A comparison of the increase in dielectric constant (Δε) from −150 to +190°C shows that for the p,p-linkage, PMDA exhibited the largest increase (e.g. ~25% at 10 kHz from ~3.4 at −150°C), followed by OPDA (23% from ~3.3), 6FDA (16% from ~3.4), and finally BTDA with the lowest increase (10% from ~3.6 at 10 kHz at −150°C) (**Figure 18a, c,** and **e**). The values of Δε decreased with increasing frequency for all four PIs and followed a decreasing order PMDA > OPDA > 6FDA > BTDA, which agreed with the trends observed in the polarization from dipole orientation determined experimentally and predicted based on a freely rotating single-dipole model. This model assumes an anti-parallel configuration for the dianhydride and diamine dipoles, such that the net dipole moment of a repeat unit is the difference between the dianhydride and diamine dipole moments without an external electric field. PMDA, being a symmetrical dianhydride, has no net dipole moment, whereas BTDA has the largest dipole moment (2.96 Debye) as a result of the benzophenone functional group. The 1.14 D dipole moment of OPDA results from the diphenyl ether, and the 2.0 D dipole moment of 6FDA from the 1,1,1,3,3,3-hexafluoropropane. The diamine portion has a dipole moment of 17.1 D which is the sum of three benzonitrile groups (4.18 D) and four diphenyl ethers (1.14 D). The largest Δε value for PMDA-based PI was accompanied by the highest dissipation factor relative to the other three PIs, but all four PIs had dissipation factor in the range of 3–8% at 190°C between 1 and 100 kHz (**Figure 18b, d,** and **f**). The results suggest that the PMDA-based PI with p,p diamine linkage had greater chain flexibility, which led to larger dipole motion at 190°C. In comparison to the p,p-linkage, the m,m-linkage resulted in a smaller increase in dielectric constant and slightly lower dissipation factor at 190°C, although the trends with respect to the dianhydrides and frequency dependence were similar. In addition, the 6FDA-based PI with m,m-linkage shows a dielectric constant of 3.1, which is noticeably lower than the p,p-linkage (ε = 3.4) and other PIs (ε ~ 3.3 to 3.6) at −150°C.

In terms of discharge energy density and efficiency, as characterized by measuring electric displacement as a function of electric field, the nitrile-containing PIs delivered 25–40% greater discharge energy density than the nitrile-free analog at an applied electric field of 100 MV/m at 190°C and frequencies of 10 Hz and 1 kHz (**Figure 19a**). For comparison, the investigators also evaluated Kapton® PI and Ultem® PEI, both of which gave similar discharge energy density to the nitrile-free PI. While the nitrile-containing PIs delivered more energy than the nitrile-free counterparts, their discharge efficiency was generally lower, as

Figure 18.
(a, c, and e) increase in dielectric constant (Δε) from −150 to +190°C and (b, d, and f) dissipation factor at 190°C at various frequencies for PIs containing three nitrile groups per diamine with various dianhydride (labeled as 3–6) and different isomeric diamine linkage (denoted as a: p,p; b: m,m; c: m,p). 3–6 represent PMDA-based, OPDA-based, 6FDA-based, and BTDA-based, respectively. Data adapted from [77].
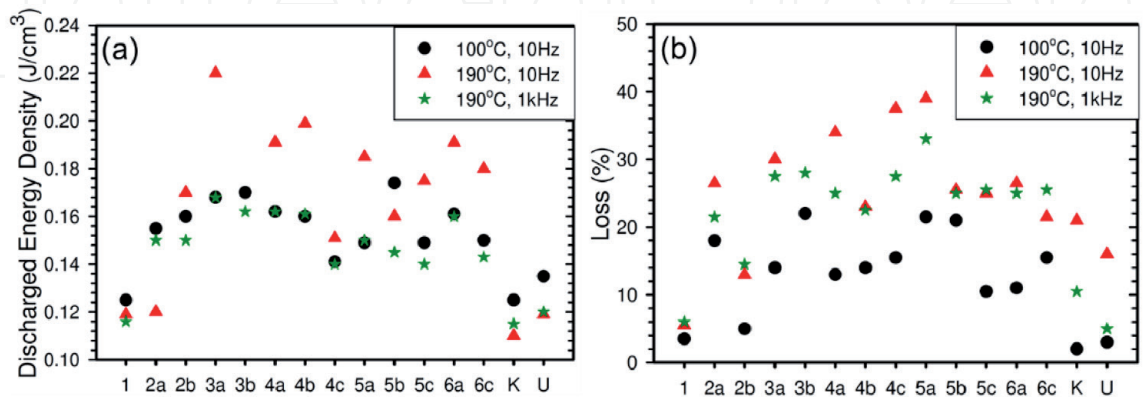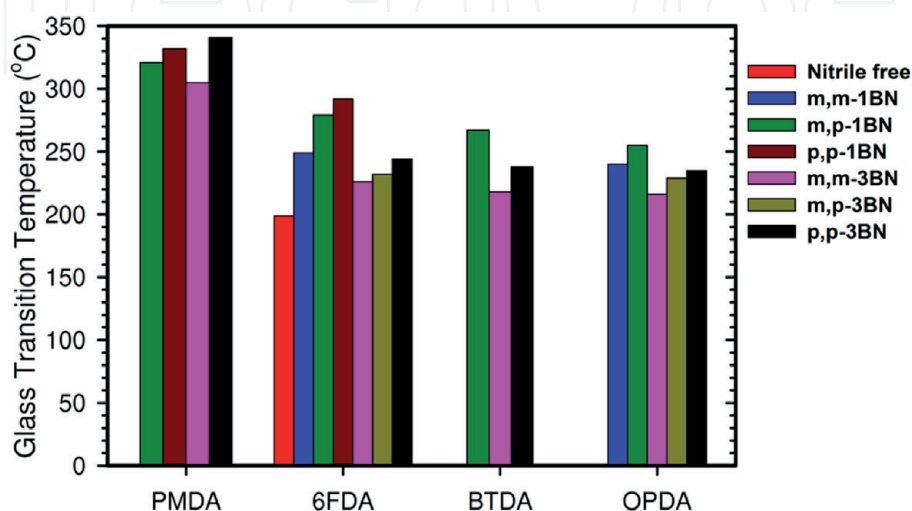

Figure 19.
*(a) Discharge energy density and (b) percent energy loss of various polyimides (PIs) at 100 MV/m at various temperatures and frequencies. PI-1 is nitrile-free 6FDA/m,m-APB (LaRC-CP2). Group 2 represents one nitrile group with OPDA. Groups 3–6 contain three nitrile groups with various dianhydrides labeled 3 as PMDA, 4 OPDA, 5 6FDA, and 6 BTDA. Labels a–c denote p,p-, m,p-, and m,m diamine linkage, respectively, while K and U represent Kapton® PI and Ultem® PEI, respectively. Electrode area: 0.05 cm².
Data adapted from [77].*

shown in **Figure 19b**. The discharge energy losses for the nitrile-containing PIs were 15–40% compared to ~5% for the nitrile-free counterpart at 190°C at 10 Hz. Kapton® PI and Ultem® PEI exhibited 15–20% loss at that temperature and frequency.

With respect to the thermal properties, based on the limited glass transition temperature (T_g) data provided by the investigators, the addition of nitrile groups in the polymer backbone appears to increase T_g, but the enhancement decreased with increasing nitrile content, as indicated by the comparison of T_g for the seven 6FDA-based PIs (**Figure 20**). The structure of the dianhydride also affects the T_g. The four PMDA-based nitrile-containing PIs appear to have the highest T_g values (300–350°C with high crystallinity), whereas the other three dianhydride families of 6FDA, BTDA, and OPDA were mostly amorphous with T_g values ranging from 220 to 300°C. By comparison, these values were at least 20°C above that of the nitrile-free LaRC-CP2 (T_g = 200°C). Additionally, the PIs with m,m diamine linkage appeared to have lower T_g than those with a p,p linkage. This effect was attributed to the greater free volume created between polymer chains by the two bent amino groups in the m,m-linkage.

An ether (—O—) linkage is another polar moiety explored for the potential enhancement in dielectric constant of PIs [80, 81]. Jeffamines® EDR-104, D230 and HK511 (**Figure 21**), which are commercial polyether aliphatic diamines, were used to introduce ether linkages into PIs. The rationale behind the use of linear alkyl diamines was to impart close-packing for reducing the overall free volume while maintaining a high density of the imide functional groups in the polymer backbone. For comparison, 1,3-diaminopropane (1,3-DAP) and 1,6-diaminohexane (1,6-DAH), were synthesized as ether-free PIs with commercial linear alkyl diamines. The dianhydrides used in the study were PDMA, BTDA, OPDA, and 6FDA. Depending on the dianhydride, the PIs with diamine D230 exhibited dielectric constants of 2.5 for 6FDA and ~4.5 for the other three dianhyrides at room temperature and 1 kHz, while those containing diamine HK511, because of the greater ether content, produced higher dielectric constants (~5.3 for PMDA and 6FDA, 6.2 for OPDA, and 7.8 for BTDA) (**Figure 22a**). Hence, the general trend for dielectric constant of the ether-containing PIs with respect to the dianhydrides followed the order BTDA ≥ OPDA > PMDA > 6FDA. The lowest dielectric constant of 2.5 observed in the PI with 6FDA/D230, was attributed to the weak electronic interaction between chains caused by the bulky CF_3 groups, which disrupted close
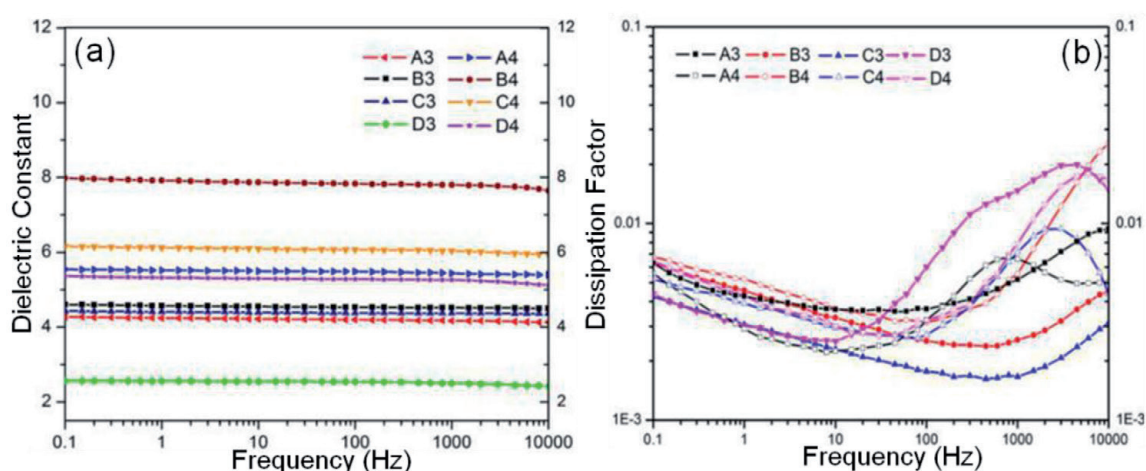

Figure 20.
Glass transition temperatures of PIs prepared from various dianhydrides: PMDA, 6FDA, BTDA, OPDA, and APB diamine isomers containing 0, 1 or 3 benzonitrile (BN) groups. Data adapted from [75–77].
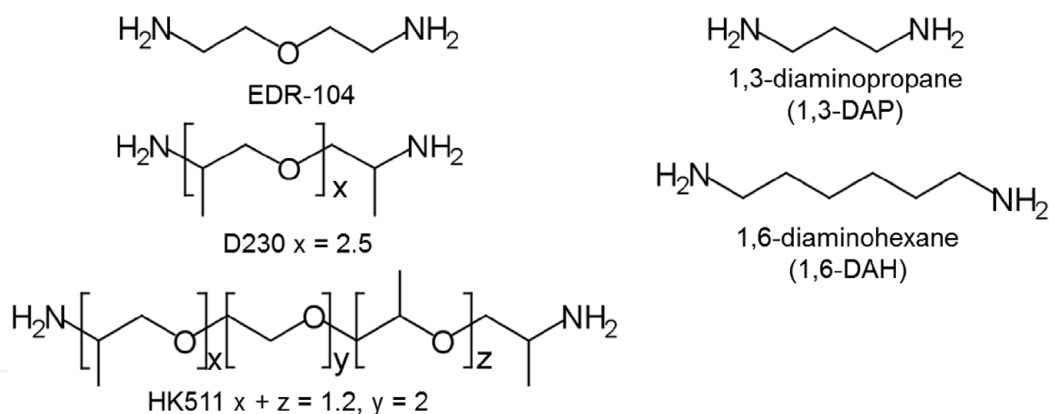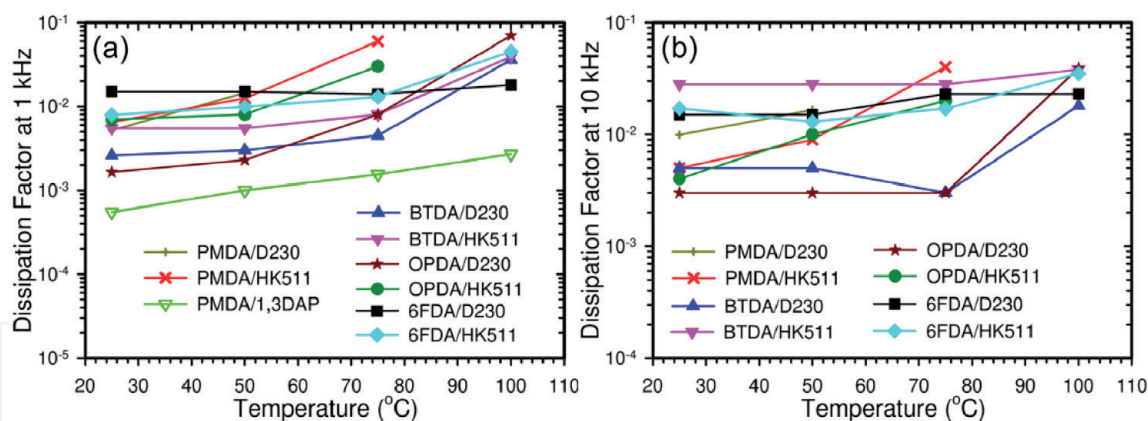
Figure 21.
Chemical structures of polyether aliphatic diamines: Jeffamines EDR-104, D230, and HK511, and linear alkyl diamines of 1,3-DAP and 1,6-DAH.

Figure 22.
(a) Dielectric constant and (b) dissipation factor at room temperature as a function of frequency for various ether-containing PIs with A–D represent PMDA, BTDA, OPDA, and 6FDA, respectively, while 3 denotes D230 polyether diamine and 4 is HK511. Figure reproduced from Figure 2 of [80] with permission from American Chemical Society.

packing. In comparison, the ether-free PIs, namely PMDA/1,3-DAP, BTDA/1,3-DAP, and BTDA/1,6-DAH exhibited dielectric constants of 5.6, 4, and 3.6, respectively. While the dielectric constants at room temperature were frequency independent in the range from 0.1 Hz to 10 kHz; the dissipation factor of the ether-containing PIs showed a strong frequency dependence with dielectric relaxation peaks of 1–2% occurring at 1 kHz and above, except for BTDA/D230 and OPDA/D230, which remained below 1% at 10 kHz (**Figure 22b**). In terms of temperature dependence, the ether-containing PIs showed almost an order of magnitude increase in dissipation factor up to 1% at frequencies of 1 kHz and 10 kHz as the temperature approached their corresponding T_g (50–100°C) (**Figure 23**). The low T_g was attributed to free volume created by the methyl side groups in the two diamines, D230 and HK511. In comparison, the two ether-free PIs, BTDA/1,3-DAP and BTDA/1,6-DAH, which were prepared from linear alkyl diamines, showed T_g of 175°C and 150°C, with crystal melting temperature of 271 and 234°C, respectively.

Another group of researchers utilized bipyridines and bipyrimidines, which are electron-rich diamines, to enhance the dielectric constant of PIs [82, 83]. The compounds of interest included 5,5′-bis(4-aminophenoxy)-2,2′-bipyridine (BPBPA) and 5,5′-bis(4-aminophenoxy)-2,2′-bipyrimidine (BAPBP) (**Figure 24**). The dianhydrides used in the study were BTDA, OPDA, PMDA, and BPDA

Figure 23.
Dissipation factor at (a) 1 kHz and (b) 10 kHz as a function of temperature for various ether-containing PIs (solid symbols) and an ether-free analog (inverted green triangle). Data adapted from [80, 81].
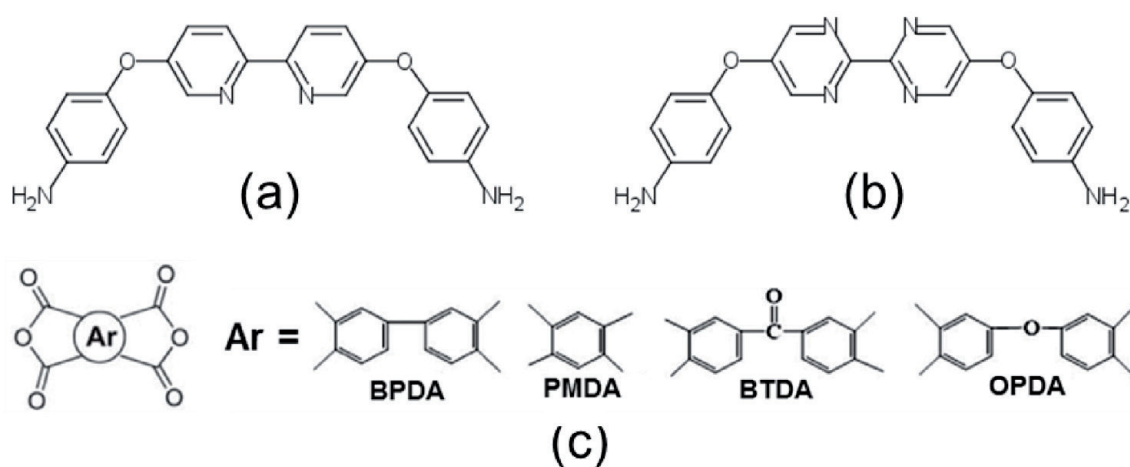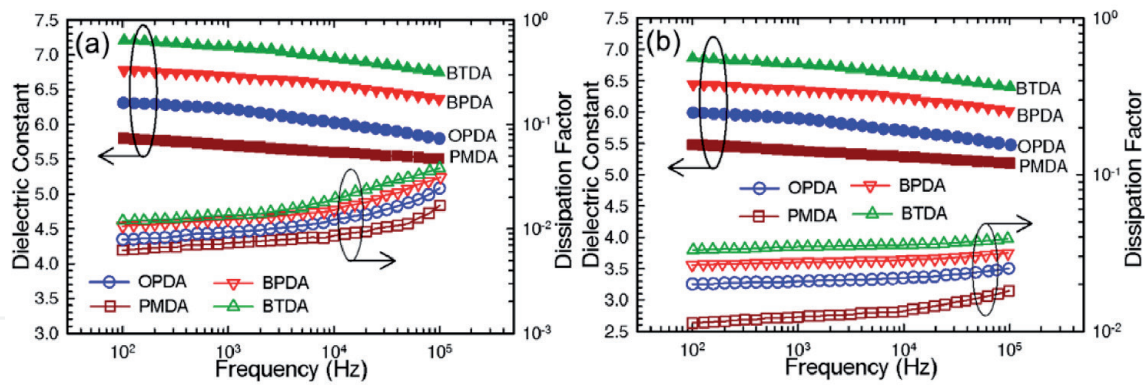

Figure 24.
Chemical structures of (a) 5,5′-bis(4-aminophenoxy)-2,2′-bipyridine (BPBPA) and (b) 5,5′-bis (4-aminophenoxy)-2,2′-bipyrimidine (BAPBP), and (c) various dianhydrides.

(3,3′,4,4′-biphenyltetracarboxylic dianhydride). The resulting PIs with BPBPA diamine possessed relatively high T_g, which differed depending on the dianhydride unit, giving a decreasing order PMDA (320°C) > BTDA (296°C) > BPDA (285°C) > OPDA (275°C). Analogously, the PI containing BAPBP diamine and BPDA dianhydride showed a T_g of 291°C. The dielectric constants for the BPBPA-based PIs ranged from ~5.5 for the PMDA-based PI to ~6.9 for the BTDA-based at room temperature and frequencies from 1 to 100 kHz, following a decreasing order of BTDA > BPDA > OPDA > PMDA (**Figure 25**). At 220°C, the dielectric constants decreased about 4% with the same decreasing trend with respect to the dianhydrides over the same frequency range. The dissipation factor for all the BPBPA-based PIs was below 4% at both room temperature and 220°C from 100 Hz to 100 kHz. For the BAPBP/BPDA PI, the dielectric response at room temperature was similar to that of the BPBPA analog.

The demand for even higher operating temperatures (~350°C) for avionics prompted researchers to develop new polymers with increased degrees of aromaticity and heterocyclic rings in the polymer backbone. In the work by Venkat et al. [84], one of the polymers synthesized was a fluorinated polyimide based on 6FDA and a diamine of 2,2-bis(4-aminophenyl) hexafluoropropane grafted with adamantane (ADE) ester pendant groups (**Figure 26**). The T_g of the PI-ADE is 305°C with a dielectric constant of 2.85–2.91 for the temperature range of 25–250°C at 10 kHz while the dissipation factor increased from 0.6% at 25°C to 0.8% at 250°C (**Figure 27**).
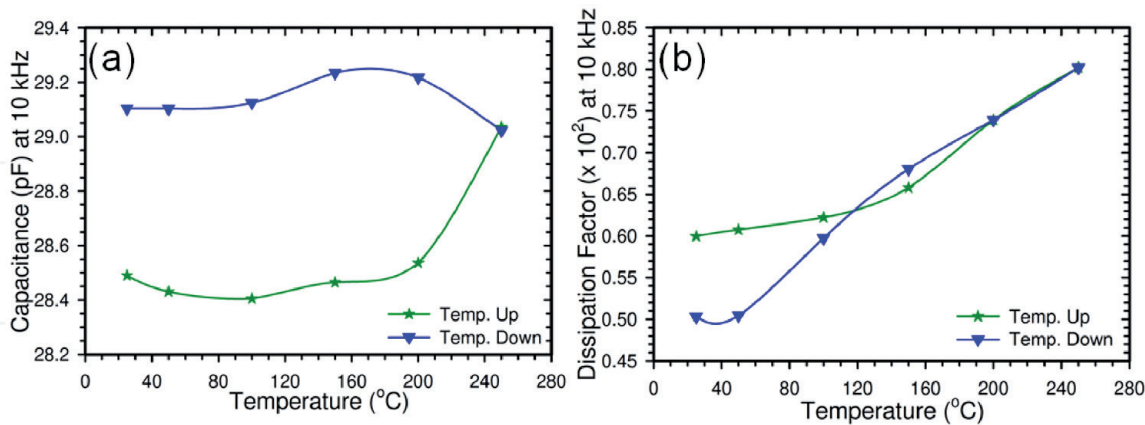
Figure 25.
Dielectric constant and dissipation factor as a function of frequency for the BPBPA-based PIs with various dianhydrides at (a) room temperature and (b) 220°C. data adapted from [82] and supporting information.
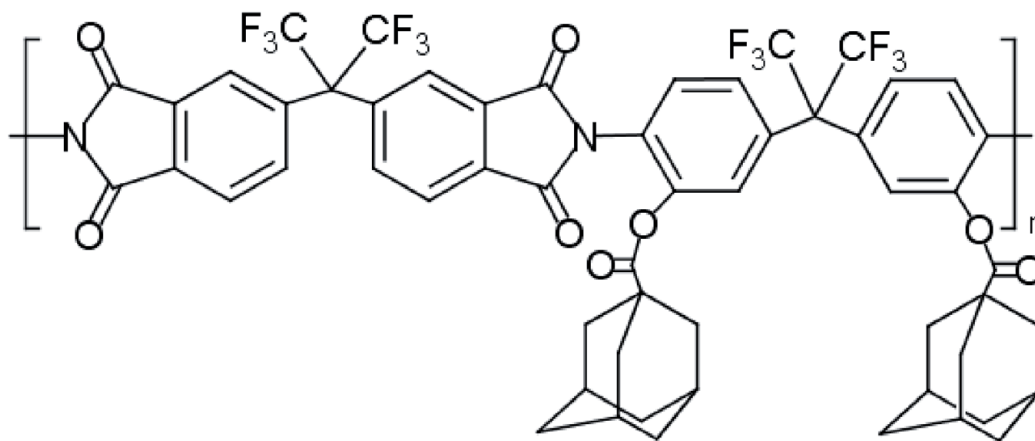
Figure 26.
Chemical structure of PI-ADE. Structures adapted from [84].

Figure 27.
Capacitance (a) and dissipation factor (b) of PI-ADE as a function of temperature at 10 kHz. Data adapted from [84].

5. Outlook

Researchers have achieved some progress in developing polyimides for capacitor dielectrics targeted for operating temperature above 150°C, but there is still major room for improvement. There is a promising new strategy of combining polymer synthesis and computational techniques (e.g., computational quantum mechanics and molecular dynamics) to synergistically search the material space for polymers

with desirable material properties (dielectric constant, glass transition temperature, etc.) for capacitor applications. The ultimate goal is to develop synthesis pathways for polymers that are as close as possible to those "discovered" through computational methods [85–89]. The synergy comes in (i) directing the focus of synthesis and (ii) providing data which simplifies characterization of synthesized polymers through computation of likely crystalline structures (with relative energy differences), IR spectra, and NMR spectra. Work in this area is still relatively limited in that some critical properties cannot be estimated through computational methods, including thermal conductivity, dielectric breakdown field (other than intrinsic), and dielectric loss at frequencies of practical interest (in the kHz region). These deficiencies in the present state of the art result in the approach being somewhat "hit or miss," but with greater guidance than conventional trial and error approaches. For example, a computational approach uncovered a new chemistry based on organotin esters that was subsequently synthesized and shown to provide greater dielectric constant than is normally available from organic polymers while maintaining a reasonable band gap [90]. This interplay between predictive modeling and synthetic chemistry will become increasingly productive with integration of additional material properties into the explored materials space, and polyimides will certainly be one material class of continued interest to researchers.

6. Concluding remarks

The use of power electronics in a growing list of high temperature and high voltage (>500 V) applications currently requires voltage derating and/or active cooling of capacitors with state of the art polymer dielectrics (such as BOPP). High temperature polymers such as polyimides offer promising advantages over the status quo by eliminating this need for voltage derating, easing thermal management requirements, and providing a failsafe for HV applications. However, the lack of commercial interest in processing some polyimides or other specialty polymers as thin films for these comparatively niche polymer applications currently limits implementation of high temperature polymers.

Acknowledgements

Conflict of interest

The authors declare no conflict of interest.

Author details

Janet Ho* and Marshall Schroeder
US Army Research Laboratory, Adelphi, MD, USA

*Address all correspondence to: janet.s.ho.civ@mail.mil

IntechOpen

References

[1] Demcko RS, editor. Evolution of high-temperature capacitors. In: 38th IEEE Electronics Components Conference, Los Angeles, CA, USA; 9-11 May 1988

[2] Dreike PL, Fleetwood DM, King DB, Sprauer DC, Zipperian TE. An overview of high-temperature electronic device technologies and potential applications. IEEE Transactions on Components, Packaging, and Manufacturing Technology-Part A. 1994;**17**(4):594-609

[3] Buttay C, Planson D, Allard B, Bergogne D, Bevilacqua P, Joubert C, et al. State of the art of high temperature power electronics. Materials Science and Engineering B. 2011;**176**(4):283-288

[4] Watson J, Castro G. High-temperature electronics pose design and reliability challenges. Analog Dialogue. 2012;**46**(7):3-9

[5] Caliari L, Bettacchi P, Boni E, Montanari D, Gamberini A, Barbieri L, et al. KEMET film capacitors for high temperature, high voltage and high current. In: CARTS International. Houston, TX, USA; 25-28 March 2013

[6] Prevallet M, Bagdy S, Prymak J, Randall M. High voltage considerations with MLCs. In: IEEE International Power Modulator Symposium and High Voltage Workshop. San Francisco, CA, USA; 23-26 May 2004

[7] Reed CW, Cichanowski SW. The fundamentals of aging in HV polymer-film capacitors. IEEE Transactions on Dielectrics and Electrical Insulation. 1994;**1**(5):904-922

[8] Boggs SA, Ho J, Jow TR. Overview of laminar dielectric capacitors. IEEE Electrical Insulation Magazine. 2010;**26**(2):7-13

[9] Gebbia M. Introduction to Film Capacitors. 2009. Available from:

https://www.illinoiscapacitor.com/pdf/Papers/introduction_to_film.pdf

[10] Weachock RJ, Liu DD. Failure analysis of dielectric breakdowns in base-metal electrode multilayer ceramic capacitors. In: CARTS International. Houston, TX, USA; 25-28 March 2013

[11] Pan M-J, Randall CA. A brief introduction to ceramic capacitors. IEEE Electrical Insulation Magazine. 2010;**26**(3):44-50

[12] Watson J, Castro G. A review of high-temperature electronics technology and applications. Journal of Materials Science: Materials in Electronics. 2015;**26**(12):9226-9235

[13] Sroog CE. History of the invention and development of the polyimides. In: Ghosh MK, Mittal KL, editors. Polyimides: Fundamentals and Applications. New York, USA: Marcel Dekker, Inc.; 1996. pp. 1-6

[14] Cozens JH. Development of plastic dielectric capacitors. IRE Transactions on Component Parts. 1959;**6**(2):114-118

[15] Carter MA. Is There a Substitute for Polycarbonate Film Capacitors? 2002. Available from: http://powerelectronics.com/site-files/powerelectronics.com/files/archive/powerelectronics.com/mag/Carter%20April%202002.pdf

[16] Critchley JP, Knight GJ, Wright WW. Polymers with heterocyclic rings in the chain: Polyimides. In: Heat-Resistant Polymers: Technologically Useful Materials. New York, USA: Plenum Press; 1983. pp. 186-258

[17] Odian G. Principles of Polymerization. 3rd ed. New York, USA: John Wiley & Sons, Inc.; 1991. p. 313

[18] Feger C, Franke H. Polyimides in high-performance electronics packaging

and optoelectronic applications. In: Ghosh MK, Mittal KL, editors. Polyimides: Fundamentals and Applications. New York, USA: Marcel Dekker, Inc.; 1996. pp. 759-814

[19] Pasquini N. Polypropylene—The business. In: Pasquini N, editor. Polypropylene Handbook. 2nd ed. Munich, Germany: Hanser; 2005. pp. 489-571

[20] DeMeuse MT. Other polymers used for biaxial films. In: DeMeuse MT, editor. Biaxial Stretching of Film: Principles and Applications. Cambridge, UK: Woodhead Publishing Limited; 2011. pp. 47-59

[21] Solvay. Ryton PPS Applications. 2020. Available from: http://www. solvay.com/en/markets-and-products/ featured-products/Ryton-Applications. html

[22] Dupont Teijin Films, Mylar PET Polyester Film and Teonex PEN Polyester Film for Use as Capacitor Dielectric. 2017. Available from: http://usa.dupontteijinfilms.com/ marketspaces/electricalcomponents/ capacitors.aspx

[23] Tekra. PEN Film Teonex Product Outline. 2020. Available from: https:// www.tekra.com/products/brands/ dupont-teijin-films/teonex

[24] Odian G. Aromatic Polysulfides. In: Principles of Polymerization. 3rd ed. New York, USA: John Wiley & Sons, Inc.; 1991. p. 158

[25] Barber P, Balasubramanian S, Anguchamy Y, Gong S, Wibowo A, Gao H, et al. Polymer composite and nanocomposite dielectric materials for pulse power energy storage. Materials. 2009;**2**(4):1697-1733

[26] Hao X. A review on the dielectric materials for high energy-storage application. Journal of Advanced Dielectrics. 2013;**3**(1):1330001

[27] Qi L, Petersson L, Liu T. Review of recent activities on dielectric films for capacitor applications. Journal of International Council on Electrical Engineering. 2014;**4**(1):1-6

[28] Chen Q, Shen Y, Zhang S, Zhang QM. Polymer-based dielectrics with high energy storage density. Annual Review of Materials Research. 2015;**45**:433-458

[29] Huan TD, Boggs S, Teyssedre G, Laurent C, Cakmak M, Kumar S, et al. Advanced polymeric dielectrics for high energy density applications. Progress in Materials Science. 2016;**83**:236-269

[30] Prateek, Thakur VK, Gupta RK. Recent progress on ferroelectric polymer-based nanocomposites for high energy density capacitors: Synthesis, dielectric properties, and future aspects. Chemical Reviews. 2016;**116**(7):4260-4317

[31] Tan D, Zhang L, Chen Q, Irwin P. High temperature capacitor polymer films. Journal of Electronic Materials. 2014;**43**(12):4569-4575

[32] Ho J, Greenbaum SG. Polymer capacitor dielectrics for high temperature applications. ACS Applied Materials & Interfaces. 2018;**10**:29189-29218

[33] Ennis JB, MacDougall FW, Yang XH, Bushnell AH, Cooper RA, Gilbert JE. High-specific-power capacitors. In: IEEE International Power Modulators and High Voltage Conference. Las Vegas, NV, USA; 27-31 May 2008

[34] Yang Y. Thermal conductivity. In: Mark JE, editor. Physical Properties of Polymers Handbook. 2nd ed. New York, USA: Springer Science+Business Media, LLC; 2007. pp. 155-164

[35] Qin S, Ho J, Rabuffi M, Borelli G, Jow TR. Implications of the anisotropic thermal conductivity of capacitor

windings. IEEE Electrical Insulation Magazine. 2011;**27**(1):7-13

[36] Li Q, Chen L, Gadinski MR, Zhang S, Zhang G, Li H, et al. Flexible high-temperature dielectric materials from polymer nanocomposites. Nature. 2015;**523**(7562):576-580

[37] Diaham S, Saysouk F, Locatelli M-L, Lebey T. Huge nanodielectric effects in polyimide/boron nitride nanocomposites revealed by the nanofiller size. Journal of Physics D: Applied Physics. 2015;**48**(38):385301

[38] Diaham S, Saysouk F, Locatelli M-L, Lebey T. Huge improvements of electrical conduction and dielectric breakdown in polyimide/BN nanocomposites. IEEE Transactions on Dielectrics and Electrical Insulation. 2016;**23**(5):2795-2803

[39] Cahill PL, Dailey JH. Aircraft Electrical Wet-Wire Arc Tracking. New Jersey, USA: US Department of Transportation/Federal Aviation Administration; August 1988. Report No.: DOT/FAA/CT-88/4

[40] Kurek J, Bernstein R, Etheridge M, LaSalle G, McMahon R, Meiner J, et al. Aircraft Wiring Degradation Study. Washington, DC: US Department of Transportation/Federal Aviation Adminstration: Raytheon Technical Services Company LLC/Federal Aviation Administration; January 2008. Report No.: DOT/FAA/AR-08/2

[41] Steinerfilm. Steinerfilm Dielectrics for Film Capacitors. 2020. Available from: http://www.steinerfilm.de/en/our-products/

[42] Smith DH, Simpson RJ, Geoghegan EDA. Final Report on Manufacturing Methods for Metallized Teflon Capacitors (Subminiature 200°C). Ohio, USA: Aeronautical Systems Division Air Force Systems Command: Dearborn Electronic

Laboratories, Inc.; 1963 April. Report No.: Technical Documentary Report Nr. ASD-TDR-63-308

[43] TDK. Film Capacitors: General Technical Information. 2018. Available from: https://en.tdk.eu/download/530754/bb7f3c742f09af6f8ef473fd34f6000e/pdf-generaltechnicalinformation.pdf

[44] Blythe AR, Bloor D. Dielectric relaxation. In: Electrical Properties of Polymers. 2nd ed. Cambridge, UK: Cambridge University Press; 2005. pp. 58-110

[45] McCrum NG, Read BE, Williams G. Phenomenological theories of mechanical and dielectric relaxation. In: Anelastic and Dielectric Effects in Polymeric Solids. New York, USA: Dover Publications, Inc.; 1991. pp. 102-140

[46] Lidow A, Strydom J, Rooij M, Reusch D. Replacing silicon power MOSFETs. In: GaN Transistors for Efficient Power Conversion. 2nd ed. West Sussex, UK: John Wiley & Sons Ltd.; 2015. pp. 232-239

[47] Cornell Dubilier Capacitors. Application Guide Snubber Capacitors. 2016. Available from: http://www.cde.com/resources/catalogs/igbtAPPguide.pdf

[48] Severns R. Design of Snubbers for Power Circuits. 2016. Available from: http://www.cde.com/resources/technical-papers/design.pdf

[49] Electrocube. High Current DC Link Film Capacitors. 2020. Available from: https://www.electrocube.com/pages/958a-series-metallized-polypropylene-dc-link-capacitors-data-sheet?_pos=10&_sid=9c2533969&_ss=r

[50] Colella T. How to Select a DC Link Capacitor. 2020. Available from: https://www.electrocube.com/pages/how-to-select-dc-link-capacitor-data-sheet

[51] Laihonen SJ, Gafvert U, Schutte T, Gedde UW. DC breakdown strength of polypropylene films: Area dependence and statistical behavior. IEEE Transactions on Dielectrics and Electrical Insulation. 2007;**14**(2):275-286

[52] Xu C, Ho J, Boggs SA. Automatic breakdown voltage measurement of polymer films. IEEE Electrical Insulation Magazine. 2008;**24**(6):30-34

[53] Schneider MA, MacDonald JR, Schalnat MC, Ennis JB. Electrical breakdown in capacitor dielectric films: Scaling laws and the role of self-healing. In: IEEE International Power Modulator and High Voltage Conference. San Diego, CA, USA; 3-7 June 2012

[54] Dissado LA, Fothergill JC. Statistical features of breakdown. In: Stevens GC, editor. Electrical Degradation and Breakdown in Polymers. London, UK: Peter Peregrinus Ltd.; 1992. pp. 319-355

[55] Blythe AR, Bloor D. Dielectric breakdown. In: Electrical Properties of Polymers. 2nd ed. Cambridge, UK: Cambridge University Press; 2005. pp. 186-216

[56] Ho J, Ramprasad R, Boggs S. Effect of alteration of antioxidant by UV treatment on the dielectric strength of BOPP capacitor film. IEEE Transactions on Dielectrics and Electrical Insulation. 2007;**14**(5):1295-1301

[57] Ho J, Jow R. Characterization of High Temperature Polymer Thin Films for Power Conditioning Capacitors. Adelphi, MD, USA: US Army Research Laboratory; 2009 July. Report No.: ARL-TR-4880

[58] Frohlich H. The theory of dielectric breakdown in solids. Proceedings of the Royal Society A. 1947;**188**(1015):521-532

[59] Simmons JG. Poole-Frenkel effect and Schottky effect in metal-insulator-metal systems. Physical Review. 1967;**155**(3):657-660

[60] Lampert MA. Current Injection in Solids. New York, USA: Academic Press; 1970

[61] Fukuma M, Nagao M, Kosaki M. Numerical analysis of dielectric breakdown in polypropylene film based on thermal and electronic composite breakdown model. In: Conference on Properties and Applications of Dielectric Materials. Tokyo, Japan; 8-12 July 1991

[62] O'Dwyer JJ, Beers BL. Thermal breakdown in dielectrics. In: Conference on Electrical Insulation and Dielectric Phenomena. Whitehaven, PA, USA; 26-28 October 1981

[63] Dissado LA, Fothergill JC. Thermal breakdown. In: Stevens GC, editor. Electrical Degradation and Breakdown in Polymers. London, UK: Peter Peregrinus Ltd.; 1992. pp. 242-262

[64] Jones RJ, Wright WF. High Temperature Polymer Dielectric Film Insulation. Aero Propulsion and Power Directorate Wright Laboratory Air Force Systems Command Wright-Patterson Air Force Base: TRW Space and Defense. Ohio, USA; 1992 February. Report No.: WL-TR-91-2105. Available from: http://www.dtic.mil/dtic/tr/fulltext/u2/a255243.pdf

[65] Jones RJ. High temperature polymer dielectric film insulation. In: 2nd NASA Workshop on Wiring for Space Applications. Cleveland, OH, USA; 6-7 October 1993

[66] Donhowe M, Lawler J, Souffie S, Lee Stein Jr E. 250°C operating temperature dielectric film capacitors. In: International Microelectronics Assembly and Packaging Society, High Temperature Electronics Network. Oxford, UK; 18-20 July 2011

[67] Vora RH, Krishnan PSG, Goh SH, Chung T-S. Synthesis and properties of designed low-k fluoro-copolyetherimides. Part I. Advanced Functional Materials. 2001;**11**(5):361-373

[68] Mandelcorn L, Miller RL. High temperature, >200 deg. C, polymer film capacitors. In: IEEE 35th International Power Sources Symposium, Cherry Hill, NJ, USA; 1992

[69] Sasaki S, Nishi S. Synthesis of fluorinated polyimides. In: Ghosh MK, Mittal KL, editors. Polyimides: Fundamentals and Applications. New York, USA: Marcel Dekker, Inc.; 1996. pp. 71-120

[70] Ghosh A, Mistri EA, Banerjee S. Fluorinated polyimides: Synthesis, properties, and applications. In: Banerjee S, editor. Handbook of Specialty Fluorinated Polymers. Massachusetts, USA: Elsevier; 2015. pp. 97-185

[71] Jones RJ, O'Rell MK, Hom JM, inventors. Polyimides Prepared from Perfluoroisopropylidene Diamine patent US 4111906; 5 September 1978

[72] Jones RJ, Chang GE, Powell SH, Green HE. Polyimide Matrix Resins for up to 700 degree F Service. Ohio, USA: TRW Engery Development Group; 1985. Report No.: N86-I1280-NTRS-NASA

[73] Kochi M, Yonezawa T, Yokota R, Mita I. Monoaxial drawing techniques for high modulus/high strength aromatic polyimide films. In: Feger C, Khojasteh MM, Htoo MS, editors. Advances in Polyimide Science and Technology. Pennsylvania, USA: Technomic Publishing Company, Inc.; 1993. p. 376

[74] Clagett DC. Engineering plastics. In: Mark HF, Bikales NM, Overberger CG, Menges G, editors. Encyclopedia of Polymer Science and Engineering. Vol. 6. New York, USA: Wiley-Interscience; 1986. pp. 94-131

[75] Wang DH, Riley JK, Fillery SP, Durstock MF, Vaia RA, Tan L-S. Synthesis and characterization of unsymmetrical benzonitrile-containing polyimides: Viscosity-lowering effect and dielectric properties. Journal of Polymer Science Part A: Polymer Chemistry. 2013;**51**:4998-5011

[76] Wang DH, Kurish BA, Treufeld I, Zhu L, Tan L-S. Synthesis and characterization of high nitrile content polyimides as dielectric films for electrical energy storage. Journal of Polymer Science Part A: Polymer Chemistry. 2015;**53**(3):422-436

[77] Treufeld I, Wang DH, Kurish BA, Tan L-S, Zhu L. Enhancing electrical energy storage using polar polyimides with nitrile groups directly attached to the main chain. Journal of Materials Chemistry A. 2014;**2**:20683-20696

[78] Clair AKS, Clair TLS, Shevket KI. Synthesis and characterization of essentially colorless polyimide films. Polymeric Materials Science and Engineering. 1984;**51**:62-66

[79] Jacobs JD, Arlen MJ, Wang DH, Ounaies Z, Berry R, Tan L-S, et al. Dielectric characteristics of polyimide CP2. Polymer. 2010;**51**:3139-3146

[80] Ma R, Baldwin AF, Wang C, Offenbach I, Cakmak M, Ramprasad R, et al. Rationally designed polyimides for high-energy density capacitor applications. ACS Applied Materials & Interfaces. 2014;**6**(13):10445-10451

[81] Baldwin AF, Ma R, Wang C, Ramprasad R, Sotzing GA. Structure-property relationship of polyimides based on pyromellitic dianhydride and short-chain aliphatic diamines for dielectric material applications. Journal of Applied Polymer Science. 2013;**130**(2):1276-1280

[82] Peng X, Wu Q, Jiang S, Hanif M, Chen S, Hou H. High dielectric constant polyimide derived from 5,5'-bis[(4-amino) phenoxy]-2,2'-bipyrimidine. Journal of Applied Polymer Science. 2014;**131**(24):40828

[83] Peng X, Xu W, Chen L, Ding Y, Xiong T, Chen S, et al. Development of high dielectric polyimides containing bipyridine units for polymer film capacitor. Reactive and Functional Polymers. 2016;**106**:93-98

[84] Venkat N, Dang TD, Bai Z, McNier VK, DeCerbo JN, Tsao B-H, et al. High temperature polymer film dielectrics for aerospace power conditioning capacitor applications. Journal of Materials Science and Engineering B. 2010;**168**(1-3):16-21

[85] Sukumar N, Krein M, Luo Q, Breneman C. MQSPR modeling in materials informatics: A way to shorten design cycles? Journal of Materials Science. 2012;**47**:7703-7715

[86] Pilania G, Wang CC, Jiang X, Rajasekaran S, Ramprasad R. Accelerating materials property predictions using machine learning. Scientific Reports. 2013;**3**

[87] Sharma V, Wang CC, Lorenzini RG, Ma R, Zhu Q, Sinkovits DW, et al. Rational design of all organic polymer dielectrics. Nature Communications. 2014;**5**:1-8

[88] Huan TD, Mannodi-Kanakkithodi A, Ramprasad R. Accelerated materials property predictions and design using motif-based fingerprints. Physical Review B. 2015;**92**:014106

[89] Wu K, Sukumar N, Lanzillo NA, Wang C, Ramprasad R, Ma R, et al. Prediction of polymer properties using infinite chain descriptors (ICD) and machine learning: Toward optimized dielectric polymeric materials. Journal of Polymer Science Part B: Polymer Physics. 2016;**54**:2082-2091

[90] Baldwin AF, Huan TD, Ma R, Mannodi-Kanakkithodi A, Tefferi M, Katz N, et al. Rational design of organotin polyesters. Macromolecules. 2015;**48**:2422-2428